

Tuning of Nanotube Mechanical Resonances by Electric Field Pulling

S. T. Purcell,* P. Vincent, C. Journet, and Vu Thien Binh

Laboratoire d'Émission Électronique, DPM UMR CNRS 5586, University Lyon-1, Villeurbanne, 69622, France

(Received 6 July 2002; published 20 December 2002)

We show here that field emission (FE) can be used to directly observe the vibration resonances ν_R of carbon nanotubes (CNTs) and that the tension created by the applied field allows the tuning of these resonances by up to a factor of 10. The resonances are observable by the changes they create in the FE pattern or the emitted FE current. The tuning is shown to be linear in voltage and to follow from the basic physics of stretched strings. The method allows one to study the mechanical properties of individual multiwall carbon nanotubes within an ensemble and follow their evolution as the CNTs are modified. The tuning and detection should be useful for nanometric resonant devices.

DOI: 10.1103/PhysRevLett.89.276103

PACS numbers: 68.65.-k, 73.63.Fg, 79.70.+q

One of the important phenomena in nanomechanics that has been recently developed for carbon nanotubes (CNTs) is the excitation of their natural mechanical resonances ν_R by an alternating electric field [1,2]. The mode forms and resonance response were directly observed by transmission electron microscopy. Besides giving a measure of the Young's modulus of an individual CNT, this has opened up applications in nanoresonant devices such as sensors, oscillator circuits, and nanobalances [1,3]. In such applications it would be useful to tune ν_R electronically. In this Letter we first present a new simple method to observe ν_R in a field emission microscope. We then show that ν_R varies simply linearly with applied voltage which creates a longitudinal tension on the CNT as in the tuning of a guitar string. ν_R was tuned at will by over 10 times its natural resonance frequency. The basic theory of the resonance phenomenon is presented and shown to be in agreement with the measurements.

A large number of multiwall carbon nanotubes (MWNTs) were grown directly by chemical vapor deposition on the end of a Ni base tip to obtain good mechanical and electrical connection. The MWNTs were straight, up to 40 μm in length, had radii in the 10–20 nm range, and were approximately aligned along the support tip axis. The Ni base tip was mounted on a heating loop which was then inserted into the classic field emission (FE) configuration in ultrahigh vacuum (10^{-10} Torr). This sample was recently used to show the existence of large heating effects accompanying FE [4]. A schema of the FE system is depicted in Fig. 1 which also illustrates how the ν_R of individual MWNTs were measured. FE electron and ion microscopy (FEM and FIM) patterns of several MWNTs were made to appear on the observation screen when the correct voltages V_A were applied to the tip. V_A was varied from -500 to -900 V for electron emission and from $+1900$ to $+2500$ V for ion imagery by argon ions at 1×10^{-4} Torr. Though many MWNTs were present on the Ni tip, the FE patterns specific to individual ones are distinguishable. This is first because FE is an

exponential function of field and hence is very selective to only a few MWNTs that are most exposed to the applied field. Second, the radial projection geometry of FE means that even if several MWNTs emit, they are in general projected at different angles and can be distinguished with ease in the FE pattern. A variable digital function generator displaying seven digits was then connected to the excitation anodes, which is actually a quadrupole, and when a ν_R was found, the corresponding part of the pattern suddenly got larger and the FE current varied. ν_R was then measured against the applied voltage to the tip for many different modes and three different MWNTs. The majority of measurements were made in the more convenient FEM mode. Note that the resonance frequency

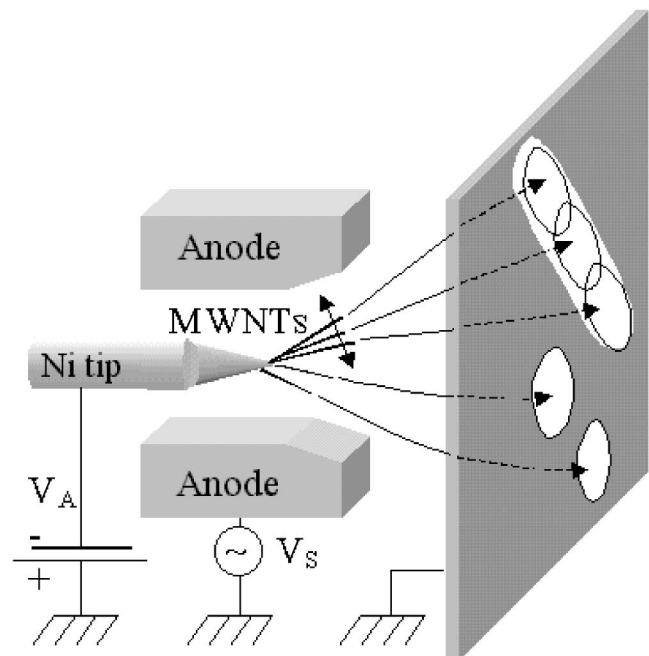


FIG. 1. Schema of the experimental field emission setup used to measure the resonances (distances: tip anode ~ 2 mm, tip screen ~ 3 cm, and screen size ~ 4 cm).

is the same as the driving frequency ν_S and not $2\nu_S$ as is possible in the TEM experiments [1,2]. This is because the driving of the large static charge induced by V_A is at least 100 times larger than that of the time varying induced charge. Different excitation amplitudes V_S were used from 0.5 to 10 V. However the true amplitudes at MHz frequencies were observed to be much smaller because of the bandpass of the anode driving system. Several FEM patterns are shown in Fig. 2(a)–2(e) that show that this method allows the easy observation of the resonances of different MWNTs of the ensemble. The irregular FEM patterns are due to imperfections in the MWNT apexes and the perturbing electrostatic fields of nearby MWNTs. The patterns are formed by FE from three different MWNTs, denoted hereafter NT1, NT2, and NT3. As ν is varied in the MHz range the individual

patterns enlarge independently as the corresponding MWNT resonates at one of its ν_R 's. The increase in pattern size gives approximately the amplitude of the CNT end angle by projection. We found angles up to as high as 20° . This experiment then permits one to distinguish absolutely if different features in a complex FE pattern are due to different CNTs. The FIM patterns of NT1 were also observed against V_A for four different resonances. This experiment detects the modes of different polarizations with the same sensitivity which is not the case in the TEM method. In Figs. 2(b) and 2(c) we show two different modes for NT1 that have approximately orthogonal directions. This is detectable in this experiment because one effectively observes the MWNTs endon. Several tens of resonances were found as ν was varied from the lowest values of 0.3 up to 20 MHz, the maximum of our generator.

The response as a function of frequency can in principle be measured by the increase in the pattern size but for now we have used the FE current, $I_{FE}(\nu)$ that is emitted from the MWNT. This was measured simultaneously to the observation of the patterns as it passes through resonance. $I_{FE}(\nu)$ varies because the average electric field, $\langle F \rangle$, at the apex of the MWNT varies when the MWNT is in resonance due to the changing of the physical position of the end of the MWNT and the resulting changes of the local average screening. Note that though $I_{FE}(\nu)$ does not give immediately the true response function because it is a function of the environment of the specific MWNT and is nonlinear in field, it does allow a good estimate of the width and form of the resonance. A typical $I_{FE}(\nu)$ curve is shown in Fig. 2(f). A feature of these measurements is that the MWNTs do not come smoothly into resonance but most often snap on or off vibration as the frequency is scanned. The quality factor Q defined here simply by $\Delta\nu/\nu$ for the central peak of this resonance is 2400. However the $I_{FE}(\nu)$ curves are most often asymmetric and the extracted values of Q vary widely for different modes, driving amplitude, and scan directions. Clearly a large number of measurements are called for to understand the response function of these MWNTs. We discuss possible mechanisms below. The measure in Fig. 2(f) shows that FE is a simple and sensitive current detection method of resonances which could be applied in nanomechanical device applications.

The result on which we concentrate in this paper is shown in Fig. 3 which is the dependence of ν_R on V_A . Plots for three pairs of different modes at the lowest frequencies found for NT1 are presented that show an almost perfect linear dependence on V_A : that is, $\nu_R(V_A) = \nu_{R0} + pV_A$ with $\nu_{R0} = 0.3$ –1 MHz and $p = 1$ –2 kHz/V. The resonances are designated as (m, n) where m designates the “type” of mode (see below) and n is the mode order. Each type m designates a specific polarization or movement of the MWNT apex and therefore a specific resonant waveform. $\nu_R(V_A)$ doubles and the polarization

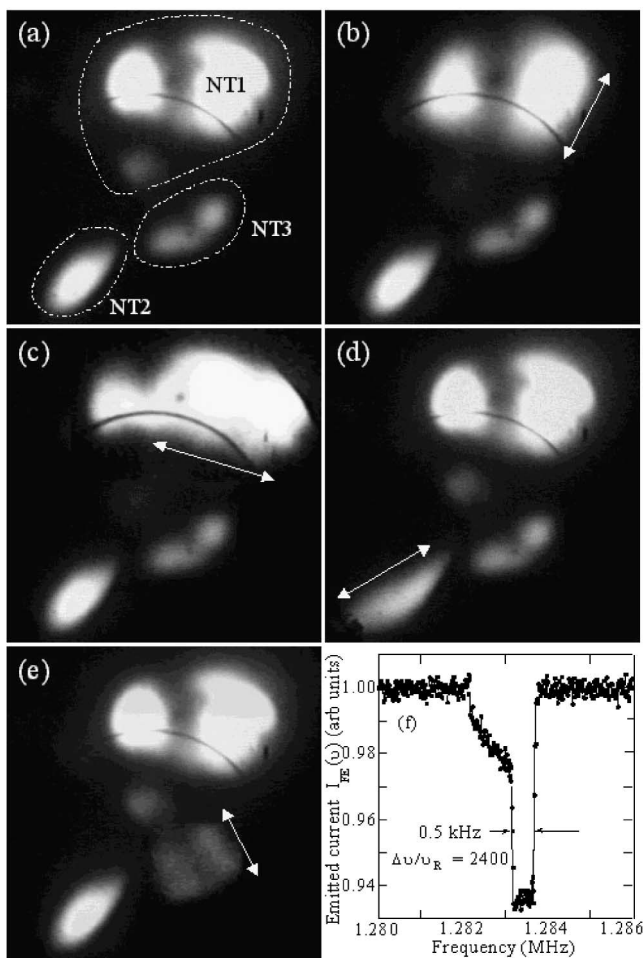


FIG. 2. $V_A = 700$ V. (a) FEM pattern out of resonance. The pattern from NT1 is overexposed so that those of NT2 and NT3 are visible. The 4 cm microchannel plate (mcp) fills most of the image. (b) NT1 in vertical resonance, $m = 2$ (see below), $\nu = 0.9588$ MHz. (c) NT1 in horizontal resonance, $m = 1$, $\nu = 0.7399$ MHz. (d) NT2 in resonance, $\nu = 0.6017$ MHz. (e) NT3 in resonance, $\nu = 1.0463$ MHz. (f) Total FE current $I_{FE}(\nu)$ as NT1 is scanned through resonance.

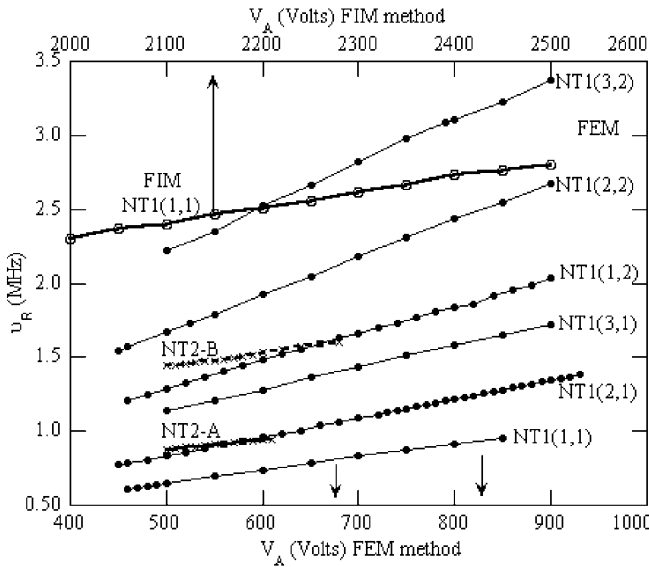


FIG. 3. Dependence of a selection of ν_R 's on V_A for NT1 and NT2. Only one measure by FIM for NT1(1,1) is shown though four series corresponding to modes (1,1) to (4,1) were measured. We find $\nu_{R0} \approx 190$ kHz and $p \approx 0.91$ kHz/V for NT1(1,1) FEM, and $\nu_{R0} \approx 280$ kHz and $p \approx 1.01$ kHz/V for NT1(1,1) FIM. They also displayed the same polarization, thus establishing the correspondence between the two series.

remained the same within each pair presented in the figure on passing from $n = 1$ to 2. The FE patterns for $m = 1$ and 2 were clearly orthogonal [see Figs. 2(b) and 2(c)] and stronger than mode $m = 3$. NT2 and NT3 also had two strong orthogonal resonances. We were not able to clearly identify higher frequency modes of NT1 with those plotted here though at least 20 other series were measured up to 10 MHz. They all showed a linear dependence on V_A with increasing ν_{R0} and p at higher frequency resonances. The polarizations were often either the same as for $n = 1$ or 2 though other mode types were also often observed. These many series are not plotted here so as not to encumber the plot. Two plots of $\nu_R(V_A)$ for NT2 are also included. ν_{R0} and p are quite different from NT1 for the same range of ν showing that we can measure the characteristic constants of different MWNTs. One plot of $\nu_R(V_A)$ for NT1(1,1) measured by FIM is also plotted which is in the 2–3 MHz range. Note that p is approximately the same in both the FIM and FEM for mode NT1(1,1) and in both cases they were the lowest frequency resonances found. Some disagreement between the two series can be expected because the high strains, particularly in the FIM mode, may create static bending effects that cause some nonlinearity in the $\nu_R(V_A)$ plots. Therefore this resonance was tuned from 0.64 to 3 MHz. Extrapolating back to $\nu_{R0} = 0.2$ –0.3 MHz, this is a factor of 10.

The linear dependence of ν_R on V_A can be understood from the basic physics of a string stretched by a tension T and that an electric field exerts a force $\propto F^2$ on a surface

where F is the electric field. We have $\nu_R \propto \sqrt{T} \alpha \sqrt{F^2} = F = \beta V_A$. β is the field amplification factor. This explains the linear dependence on V_A . In more detail, T is created only by the longitudinal force at the MWNT cap given by $T = (\epsilon_0/2) \int F^2 \hat{z} \cdot d\mathbf{A}$ where z is along the MWNT axis. Depending on the shape of the cap, T is a fraction of $T_0 \equiv (\epsilon_0/2) \pi r^2 F_0^2 = (\pi \epsilon_0/2) (r \beta_0 V_A)^2$ where F_0 and β_0 are the maximum values of F and β in the emission zone and r is the radius of the MWNT. For a smooth hemispherical cap we used the field distributions given by Dyke and Dolan [5] to calculate this fraction to be $T = 0.64 T_0$. For an uneven cap as in our case it can be much smaller. We write formally:

$$T \cong (\pi \epsilon_0/2) (r_e \beta_0 V_A)^2 \equiv \gamma^2 V_A^2, \quad (1)$$

where r_e is an effective radius of the emission zone.

The equation for a rigid stretched string is [6]

$$\frac{\partial^2 y}{\partial t^2} = \frac{T}{\rho_L} \frac{\partial^2 y}{\partial x^2} - \frac{EI}{\rho_L} \frac{\partial^4 y}{\partial x^4}, \quad (2)$$

with ρ_L the mass per unit length, E the Young's modulus, and $I \cong (\pi/4)r^4$ the "cross sectional area moment of inertia," neglecting the hollow inner tube diameter. The method for deriving the general waveform and resonance condition can be found in many texts and is rather cumbersome [6]. In our limit the tension term is larger than the rigidity, or $T \gg (n\pi/L)EI$. After some work the condition is rather simple and in the desired form:

$$\begin{aligned} \nu_R(V_A) &\cong \nu_{R0} + pV_A; & \nu_{R0} &= \frac{n}{L^2} \sqrt{\frac{EI}{\rho_L}}; \\ p &= \frac{n\gamma}{2L} \sqrt{\frac{1}{\rho_L}}. \end{aligned} \quad (3)$$

The resonance is linear in n , the y offset depends only on the mechanical properties of the tube, and the tension term is linear in V_A . Note that the form of ν_{R0} here is not the same as in rigid strings at zero tension [1] as a different mathematical limit applies. For these first measures we have only rough estimates of L and r for the MWNTs so we prove here only that we have an order of magnitude agreement with the formulas. We take $r = 10$ –25 nm, $L = 10$ –40 μm , $E = 10^{10}$ – 10^{12} Pa [7], and the density of graphite = 2.26 kg/m³. This gives a wide range of $\nu_{R0} = 5 \times 10^3$ – 2×10^6 Hz into which the measurements fall (0.2–0.4 MHz for $m = 1$). In the second term the unknown is r_e . FE onset occurred at 500 V for which we must have $F_0 \sim 3$ V/nm to allow FE. This gives $\beta_0 \approx 7 \times 10^6$ m⁻¹. From the plots $p \cong 1$ kHz/V for $n = 1$. For the range of L and r given above this gives $r_e \sim 1$ –10 nm which is in the expected range.

From the above discussion it seems clear that we understand the basic mechanism of the resonance tuning. One aspect of the measurements that deserves mention is the multiplicity of different modes and mode types. These

modes are not the driving of a perfect MWNT in controlled directions but the excitation of the characteristic modes of our nonhomogeneous MWNTs. Different polarization modes have already been observed by Wang *et al.* [8] and ascribed to the mechanical anisotropies in their nanotubes. The large number of modes observed here may therefore be due to a combination of the nonhomogeneity of our MWNTs, the close proximity of other MWNTs which may also go into resonance, the symmetry breaking electrostatic force of V_A , and of course the excitation of higher order modes. Another interesting aspect is the tendency of the tubes to snap into and out of resonance reversibly while scanning ν [see Fig. 2(f)]. One explanation is that from classical physics nonlinear driving creates abrupt transitions in the frequency response function [6]. It is also possible that the vibrations may create reversible configurations in the MWNT structure as has been observed and theoretically modeled [9] for single wall CNTs. From a practical point of view, the abrupt breaks in $I_{FE}(\nu)$ allow the detection of a change in the ν_R much finer than predicted by the Q .

There are numerous ramifications of this work. This is a new and simple method to measure the mechanical resonances of CNTs. This is a standard geometry for FE studies used currently by hundreds of researchers worldwide. They need only to add a function generator to study the mechanical properties of their CNTs. The technique allows a clear identification of different CNTs within a complex FE pattern. The mechanical properties can be followed as the CNTs evolve under FE which permits recrystallization, tube shortening, and narrowing by evaporation, deposition, ion bombardment, oxidation, etc. The FE current sensing can provide feedback signals for nanoresonating devices. It is easy to show that electric force can create strains of up to $\sim 1\%$. Thus one can carry out stress-strain experiments to influence the microscopic and macroscopic structure of the CNTs and which in turn can be immediately followed by the resonance experiments.

The wide range electronic tuning can be used for nano-electromechanical systems, for example, for the tuning of arrayed CNTs to have the same frequency or in resonant atomic force experiments. In this experiment the field was applied at the tube end. A transversal static field will also create similar tuning for circuits in which the CNT is fixed at both ends. An exotic application comes from the fact that ν_R is sensitive to the area and field at the apex of

the CNT. Therefore at high fields the addition of one atom to the cap of a smooth CNT will shift ν_R by $\sim \sqrt{dA/A}$ where dA is the “size” of the added atom. For a (10,10) single wall CNT of 30 end atoms this is $\sim 1\%–2\%$. The high Q resonances should easily detect the arrival of single atoms. This is a sensitivity of the mechanical resonance of the CNT up to 12 orders of magnitude less atoms than reported for the nanobalance [1].

Finally, we have recently shown that FE permits the controlled heating of individual MWNTs up to 2000 K by Joule heating along the MWNT and quantitative measurements of the induced temperature and MWNT resistance [4]. This was done in the same FE setup used here. In parallel with modelization [10] and microscopy studies of the MWNT dimensions one can estimate the electrical and thermal conductivities, σ and κ . It is therefore now possible to have access to σ , κ , and E for a single nanotube, or other nanowires, in a single experimental setup at any stage in their evolution.

*Electronic address: purcell@dpm.univ-lyon1.fr

- [1] P. Poncharal, Z. L. Wang, D. Ugarte, and W. A. de Heer, *Science* **283**, 1513 (1999).
- [2] R. Gao, Z. L. Wang, Z. Bai, W. A. de Heer, L. Dai, and M. Gao, *Phys. Rev. Lett.* **85**, 622 (2000).
- [3] See D. Qian, G. J. Wagner, W. K. Liu, M.-F. Yu, and R. S. Ruoff, *Appl. Mech. Rev.* **55**, 495 (2002).
- [4] S. T. Purcell, P. Vincent, C. Journet, and Vu Thien Binh, *Phys. Rev. Lett.*, **88**, 105502 (2002).
- [5] W. P. Dyke and W. W. Dolan, in *Field Emission*, edited by L. Marton, *Advances in Electronics and Electron Physics* Vol. 8 (Academic Press, New York, 1956).
- [6] L. Meirovitch, *Elements of Vibration Analysis* (McGraw-Hill, New York, 1986); C. Vallette, *Mecanique de la Corde Vibrante* (Hermes, Paris, 1993) (in French).
- [7] M. M. J. Treacy, T. W. Ebbesen, and J. M. Gibson, *Nature (London)* **381**, 678 (1996); J.-P. Salvetat, A. J. Kulik, J.-M. Bonard, G. Briggs, T. Stöckli, K. Méténier, S. Bonnamy, F. Béguin, N. A. Burnham, and L. Forro, *Adv. Mater.* **11**, 161 (1999).
- [8] Z. L. Wang, R. P. Gao, P. Poncharal, W. A. de Heer, Z. R. Dai, and Z. W. Pan, *Mater. Sci. Eng., C* **16**, 3 (2001).
- [9] S. Iijima, C. Brabec, A. Maiti, and J. Bernholc, *J. Chem. Phys.* **104**, 2089 (1995); B. I. Yakobson, C. J. Brabec, and J. Bernholc, *Phys. Rev. Lett.* **76**, 2511 (1996).
- [10] P. Vincent, S. T. Purcell, C. Journet, and Vu Thien Binh, *Phys. Rev. B* **66**, 075406 (2002).